

ON THE DRAWING IN ULTRASONIC FIELD OF METALLIC WIRES WITH HIGH MECHANICAL RESISTANCE

M. Susan, L. Gh. Bujoreanu*, D. G. Gălușcă, C. Munteanu, M. Mantu

Faculty of Materials Science and Engineering, the "Gh. Asachi" Technical University from Iași, Bd. D. Mangeron 63, 700050 Iași

The paper introduces ultrasonic vibration drawing (UVD) as a new technology for processing high mechanical resistance wires. A calculation method has been developed for the drawing force based on the theorem of total consumed power, considering a spherical rate field, a static flow, a Coulomb-type friction and the existence of the "reversion mechanism of average friction force" at metal-tool contact when the die is located in the oscillation maxima of the waves and ultrasonically actuated along drawing direction. Analytical results were in good agreement with experimental results obtained on ball-bearing steel wires. The advantages of UVD technology as compared to classical technology (CT) have been emphasized by means of the mechanical characteristics of resistance and plasticity determined from tensile tests of the correspondingly processed wires.

(Received August 18, 2004; accepted March 23, 2005)

Keywords: Wire drawing, Ultrasonics, Spherical rate field, Laminar flow, Efficiency

1. Introduction

Metallic wires are generally obtained by cold drawing, a technology that is also called wire drawing. Plastic deformation by wire drawing is accompanied by work hardening, involving the rise of mechanical characteristics of resistance and the diminishing of mechanical characteristics of plasticity. In the case of high resistance wires, work hardening is more intense, which renders cold processing much more difficult [1].

In order to accomplish the processing of high mechanical resistance metallic wires, the present paper introduces ultrasonic vibration drawing (UVD) as an alternative to classical technology (CT). For a more comprehensive characterization of UVD technology as compared to CT, three main aspects are treated: (i) calculation of the rate field and the drawing force; (ii) experiments performed on ball-bearing wires and (iii) analysis of UVD effects on mechanical characteristics of resistance and plasticity of the processed wires.

2. Calculation of rate field and drawing force at wire processing in ultrasonic field, according to UVD technology

Within UVD technology wire processing is performed with the die located in the oscillation maxima of the waves and actuated along drawing direction. The principle scheme of UVD technology is shown in Fig. 1.

Conical convergent dies were used with a cylindrical calibration zone of the processed wire. Any given point M, from the deformation zone, takes part to two motions: a feed motion with v_s rate along the generator of the deformation cone and a vibratory motion with v_v rate. The resulting vector of relative rate (after composing the two rate vectors) will change the displacement sense of point M as follows: during $T/2 - 2t_1$ its displacement sense will coincide with that of the metal and during

* Corresponding author: lgbujor@tuiasi.ro

$T/2 + 2t_1$ the displacement will be done in contrary sense. This supposition explains, in fact, the “reversion mechanism of average friction force” at the metal-tool contact, assuming a Coulomb-type friction.

When wires with high mechanical resistance are processed, the semi-angle of deformation cone must be $\alpha \leq 10^\circ$ [1]. Since $v_s = v_{dr} \cos \alpha$, it is a good technological approximation to consider $v_s \approx v_{dr}$, the drawing rate. The “reversion mechanism of average friction force”, at metal-tool contact, has been previously detailed [2] and the friction coefficient in case of applying UVD technology to wires with cylindrical symmetry has been determined as:

$$\mu^{UVD} = \mu^{CT} \left(1 - \frac{2}{\pi} \arccos \frac{v_{dr}}{v_v} \right) \quad (1)$$

where $\left| \frac{v_{dr}}{v_v} \right| \leq 1$ and μ^{CT} is the friction coefficient at classical technology.

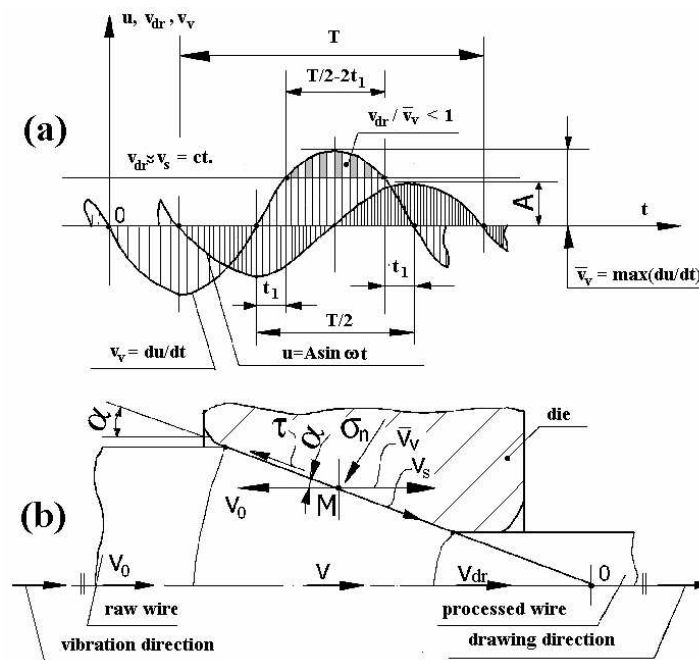


Fig. 1. Principle scheme of UVD technology: (a) variation in time of wave displacement (u), drawing rate (v_{dr}) and vibration rate (v_v); (b) proper scheme: σ_n - normal stress in any given point M , τ - shear stress on metal-tool interface, v_s - slip rate of metal during drawing, v_v - maximum vibration rate of the die, α - semi angle of deformation cone, v_0 - initial rate (raw wire), v_{dr} - final drawing rate (processed wire), A - oscillation amplitude.

2.1 The rate field at wire drawing

The calculation of drawing stress is based on the rate field [1, 3] illustrated in Fig. 2. The hypotheses of plastic deformation are [1,3,4]: (i) the metallic material is incompressible; (ii) the die is a rigid body; (iii) the material deformation is performed according to Von Mises flow condition; (iv) the rate field provides a Bernoulli-type continuity; (v) the Coulomb-type metal-tool contact friction is constant for a given drawing process; (vi) on the oscillating system only longitudinal elastic waves are acting in stationary regime and (vii) the deformation process is isothermal.

In the areas I and III the rate is uniform and has only axial components with the magnitudes v_0 and v_{dr} , respectively which, due to the constancy of metal flow, are interdependent:

$$v_0 = v_{dr} (R_1/R_0)^2 \quad (2)$$

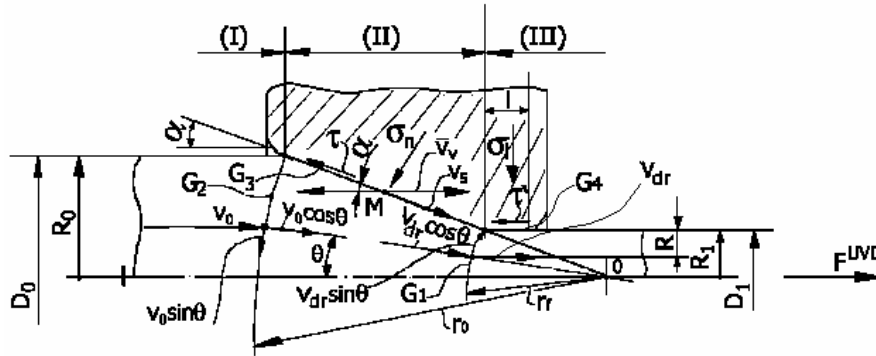


Fig. 2. Rate field in the deformation area: R_0, D_0 – dimensions of raw wire; R_1, D_1 – dimensions of processed wire; σ_n – normal stress within the calibration area of the die; τ – shear stress within the calibration area of the die; F^{LVD} – drawing force; l – length of the calibration area of the die.

The area of plastic deformation II is bounded by two spherical surfaces, G_1 of radius r_f and G_2 of radius r_0 and by a conical surface G_3 defined by the angle 2α and limited to the right by the cylindrical surface G_4 . In this area the rate is oriented towards the cone's tip, O , and has cylindrical symmetry. In spherical coordinates, (r, θ, φ) the components of the displacement rate are determined as displacement derivatives as a function of time ($\dot{u}_r, \dot{u}_\theta, \dot{u}_\varphi$). The components of deformation rate are determined as derivatives of the deformation degree as a function of time, as follows [1]:

$$\left\{ \begin{aligned} \dot{\epsilon}_{rr} &= \partial \dot{u}_r / \partial r \\ \dot{\epsilon}_{\theta\theta} &= (1/r)(\partial \dot{u}_\theta / \partial \theta) + \dot{u}_r / r \\ \dot{\epsilon}_{\varphi\varphi} &= (1/r \sin \theta)(\partial \dot{u}_\varphi / \partial \varphi) + (\dot{u}_r / r) + (\dot{u}_\theta / r) \cot \theta \\ \dot{\epsilon}_{r\theta} &= (1/2)[(\partial \dot{u}_\theta / \partial r) - (\dot{u}_\theta / r) + (1/r)(\partial \dot{u}_r / \partial \theta)] \\ \dot{\epsilon}_{\theta\varphi} &= (1/2)[(1/r \sin \theta)(\partial \dot{u}_\theta / \partial \varphi) + (1/r)(\partial \dot{u}_\varphi / \partial \theta) - (\dot{u}_\varphi / r) \cot \theta] \\ \dot{\epsilon}_{\varphi r} &= (1/2)[(\partial \dot{u}_r / \partial r) - (\dot{u}_\varphi / r) - (1/r \sin \theta)(\partial \dot{u}_r / \partial \varphi)] \end{aligned} \right. \quad (3)$$

Since the volume element is in equilibrium, the following equation system is obtained:

$$\left\{ \begin{aligned} \frac{\partial \sigma_{rr}}{\partial r} + \frac{1}{r \sin \theta} \cdot \frac{\partial \sigma_{r\varphi}}{\partial \varphi} + \frac{1}{r} \cdot \frac{\partial \sigma_{r\theta}}{\partial \theta} + \frac{2\sigma_{rr} - \sigma_{\theta\theta} - \sigma_{\varphi\varphi} + \sigma_{r\theta} \cot \theta}{r} &= 0 \\ \frac{\partial \sigma_{r\theta}}{\partial r} + \frac{1}{r \sin \theta} \cdot \frac{\partial \sigma_{\varphi\theta}}{\partial \varphi} + \frac{1}{r} \cdot \frac{\partial \sigma_{\theta\theta}}{\partial \theta} + \frac{3\sigma_{r\theta} + (\sigma_{\theta\theta} - \sigma_{\varphi\varphi}) \cot \theta}{r} &= 0 \\ \frac{\partial \sigma_{r\varphi}}{\partial r} + \frac{1}{r \sin \theta} \cdot \frac{\partial \sigma_{\varphi\varphi}}{\partial \varphi} + \frac{1}{r} \cdot \frac{\partial \sigma_{\varphi\theta}}{\partial \theta} + \frac{3\sigma_{r\varphi} + \sigma_{\varphi\theta} \cot \theta}{r} &= 0 \end{aligned} \right. \quad (4)$$

The components of displacement rate in zone II are:

$$\left\{ \begin{aligned} \dot{u}_r &= v = v_{dr} r_f^2 (\cos \theta / r_0^2) \\ \dot{u}_\theta &= \dot{u}_\varphi = 0 \end{aligned} \right. \quad (5)$$

Along the G_1 and G_2 limits, the normal components of rate are continuous; however rate discontinuities occur at parallel positions to these limits, having the expression, for G_1 :

$$\Delta v_1 = v_{dr} \sin \theta, \quad (6)$$

and for G_2 :

$$\Delta v_2 = v_0 \sin \theta \quad (7)$$

Since the die is a rigid body, rate discontinuities occur both on G_3 conical surface, as:

$$\Delta v_3 = v_{dr} r_f^2 (\cos \alpha / r_0^2) \quad (8)$$

and on G_4 cylindrical surface as:

$$\Delta v_4 = v_{dr} \quad (9)$$

Under these circumstances, the volumetric rate \dot{V} of metal flow through any surface bounded by the conical tubular channel defined by $d\theta$ has to be identical to the rate of the metal flow through the elementary tube defined by dR . It is obvious that in the area III: $R = r_f \sin \theta$, therefore $dR = r_f \cos \theta \cdot d\theta$, which gives the volumetric rate of metal flow through area III:

$$\dot{V}_3 = 2\pi R dR v_{dr} = 2\pi v_{dr} r_f^2 \sin \theta \cos \theta \cdot d\theta \quad (10)$$

Likewise, in area II the volumetric rate will be:

$$\dot{V}_2 = -2\pi r \sin \theta \cdot r \cdot d\theta \cdot u_r \quad (11)$$

From the equality of the two volumetric rates, \dot{V}_2 and \dot{V}_3 it follows:

$$u_r = -v_{dr} r_f^2 (\cos \theta / r_0^2) \quad (12)$$

2.2 The drawing force

The drawing force can be determined based on total consumed power (\dot{W}_{tot}) considering the spherical rate field illustrated in Fig. 2 that provides a Bernoulli-type continuity of the metal flow. Besides the power consumed for proper plastic deformation (\dot{W}_{def}), total consumed power also considers the power (\dot{W}_{SG}) lost by friction on surfaces G_3 and G_4 and owing to the rate discontinuities when crossing the surfaces G_1 and G_2 :

$$\dot{W}_{tot} = \dot{W}_{def} + \dot{W}_{SG} \quad (13)$$

The power necessary for plastic deformation by drawing has the expression:

$$\dot{W}_{nec} = \pi v_{dr} R_1^2 \sigma_{an}^{UVD} \quad (14)$$

and has to balance total power consumption. The plastic deformation of material occurs only in the area II. Owing to the axial-cylindrical symmetry as a function of φ , equation system (3) becomes:

$$\left\{ \begin{array}{l} \dot{\epsilon}_{rr} = \partial u_r / \partial \theta \\ \dot{\epsilon}_{\theta\theta} = u_r / r \\ \dot{\epsilon}_{\varphi\varphi} = u_r / r \\ \dot{\epsilon}_{r\theta} = (1/2r)[(\partial u_\theta / \partial \theta)] \\ \dot{\epsilon}_{\theta\varphi} = \dot{\epsilon}_{r\varphi} = 0 \end{array} \right. \quad (15)$$

Considering the rate field equations given by relationship (5) the deformation rates become:

$$\left\{ \begin{array}{l} \dot{\epsilon}_{rr} = -2\dot{\epsilon}_{\theta\theta} = -2\dot{\epsilon}_{\varphi\varphi} = 2v_{dr} r_f^2 (\cos \theta / r_0^3) \\ \dot{\epsilon}_{r\theta} = (1/2r)v_{dr} r_f^2 (\sin \theta / r_0^3) \\ \dot{\epsilon}_{\theta\varphi} = \dot{\epsilon}_{r\varphi} = 0 \end{array} \right. \quad (16)$$

Therefore, the power consumed for proper deformation (\dot{W}_{def}) has the expression:

$$\dot{W}_{\text{def}} = (2/\sqrt{3}) \cdot \sigma_c \cdot \int_V \sqrt{(1/2)(\dot{\epsilon}_{ij} \cdot \dot{\epsilon}_{ji})} dV \quad (17)$$

where $dV = 2\pi r \cdot \sin\theta \cdot r d\theta \cdot dr$.

Performing the corresponding calculations, considering the integration limits $\theta = 0 \rightarrow \alpha$ and $r = r_f \rightarrow r_0$ and the relationships $r_0/r_f = R_0/R_1$ and $r_f = R_1(1/\sin\alpha)$ it follows that \dot{W}_{def} has the expression [1]:

$$\dot{W}_{\text{def}} = (2\pi\sigma_c \cdot v_{\text{dr}} R_1^2 f_{(\alpha)} \cdot \ln(R_0/R_1)) \quad (18)$$

where:

$$f_{(\alpha)} = (1/\sin^2 \alpha) [1 - \cos \alpha \sqrt{1 - (11/12) \sin^2 \alpha} + \frac{1}{\sqrt{11 \cdot 12}} \ln \frac{1 + \sqrt{11/12}}{(\sqrt{11/12}) \cos \alpha + \sqrt{1 - (11/12) \sin^2 \alpha}}] \quad (19)$$

Due to rate discontinuities, power losses occur on surfaces G_1 and G_2 . The condition of metal flow continuity requires the normal components of rate, derived from each of the rate fields on these surfaces, to be equivalent. Thus the normal component, acting on the left side of the G_1 surface in Fig. 2, has the expression:

$$\dot{u}_r = v_{\text{dr}} \cos \theta \quad (20)$$

In the same way, the axial component of v_{dr} rate in area III, normal on G_1 surface, has the same value, $v_{\text{dr}} \cos \theta$. On the other hand, tangential components are no longer equal, the difference being also called rate discontinuity.

Based on Von Mises flowing criterion, the power consumed along the surfaces G_1 and G_2 has the expression:

$$\dot{W}_{SG_1, G_2} = \int_{G_1, G_2} \tau \Delta v dS = \int_{G_1} \tau \Delta v_1 dS + \int_{G_2} \tau \Delta v_2 dS = 4\pi v_{\text{dr}} r_f^2 (\sigma_c / \sqrt{3}) \int_{\theta=0}^{\alpha} \sin^2 \theta d\theta \quad (21)$$

After integration, \dot{W}_{SG_1, G_2} becomes:

$$\dot{W}_{SG_1, G_2} = (2/\sqrt{3}) \sigma_c \pi v_{\text{dr}} r_f^2 (\alpha - \sin \alpha \cos \alpha) = (2/\sqrt{3}) \sigma_c \pi v_{\text{dr}} R_1^2 [(\alpha/\sin^2 \alpha) - \cot \alpha] \quad (22)$$

The power losses caused by the friction between metal and tool are consumed at the level of the surfaces G_3 and G_4 .

Along the conical portion, bounded by G_3 surface, the rate discontinuity (Δv_3) is given by the relationship:

$$\Delta v_3 = v_{\text{dr}} (r_f^2 / r_0^2) \cos \alpha = v_{\text{dr}} (R_1 / R_0)^2 \cos \alpha \quad (23)$$

and the contact surface element is $dS = 2\pi r (dR / \sin \alpha)$.

At the level of G_4 cylindrical surface the rate discontinuity is $\Delta v_4 = v_{\text{dr}}$.

Considering Sach's relationship as $\sigma_n = \sigma_c [\ln(R_0/R_1)^2 - 1]$, the following expressions are obtained for

\dot{W}_{SG_3} and \dot{W}_{SG_4} power losses by friction:

$$\dot{W}_{SG_3} = \int_{G_3} \tau \Delta v_3 dS = 2\pi \mu^{UVD} v_{\text{dr}} R_1^2 \cot \alpha [1 - \ln(R_0/R_1)] \sigma_c \ln(R_0/R_1) \quad (24)$$

and:

$$\dot{W}_{SG_4} = \int_{G_4} \tau \Delta v_4 dS = 2\pi \mu^{UVD} v_{\text{dr}} R_1^2 (1/R_1) (\sigma_c - \sigma_{\text{an}}^{UVD}) \quad (25)$$

In relationships (24) and (25) the friction coefficient for UVD technology is given by (1). From the power balance it follows that the drawing stress σ^{UVD} has the analytical expression:

$$\begin{aligned} \sigma_{an}^{UVD} = & \sigma_c \{ 2f_{(\alpha)} \ln(R_0/R_1) + (2/\sqrt{3})[(\alpha/\sin^2 \alpha) - \cot \alpha] \} + \\ & + 2\mu^{UVD} [\cot \alpha [1 - \ln(R_0/R_1)] \ln(R_0/R_1) + 1/R_1] / [1 + 2\mu^{UVD} (1/R_1)] \end{aligned} \quad (26)$$

which gives:

$$\begin{aligned} \sigma_{an}^{UVD} = & \sigma_c \{ 2f_{(\alpha)} \ln(R_0/R_1) + (2/\sqrt{3})[(\alpha/\sin^2 \alpha) - \cot \alpha] \} + \\ & + [\cot \alpha [1 - \ln(R_0/R_1)] \ln(R_0/R_1) + 1/R_1] \cdot [2\mu^{UVD} / (1 + \mu^{UVD} R_0/R_1)] \end{aligned} \quad (27)$$

The drawing force is determined by:

$$F_{an}^{UVD} = S_1 \sigma_{an}^{UVD} = 1/4 \cdot \pi D_1^2 \sigma_{an}^{UVD} \quad (28)$$

In the above S_1 represents the processed wire cross section and $f_{(\alpha)}$ is given by (19).

3. Experimental procedure

The experiments were performed on a classical hydraulically actuated drawing bench able to develop a drawing force of 12×10^4 N and an active stroke of 1.5 m. The assembly of the oscillating system has been fastened on the resistance frame of the bench by means of the nodal flange. The principle scheme of the experimental installation, used for wire drawing in ultrasonic field is illustrated in Fig. 3.

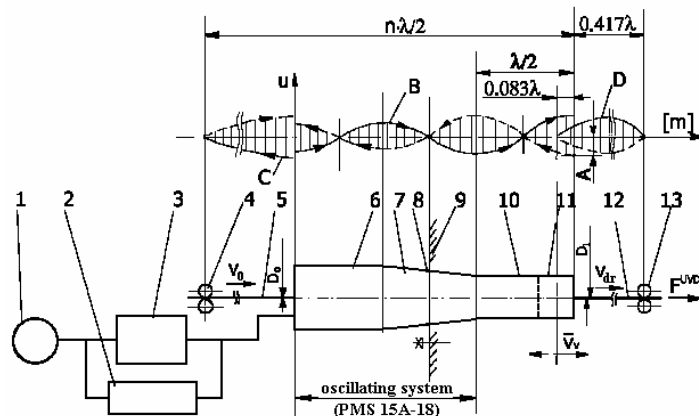


Fig. 3. Principle scheme of the experimental installation used for wire drawing in ultrasonic field, according to UVD technology: 1 – supply bloc; 2 – polarization bloc; 3 – ultrasonics generator type UZG 2-4M; 4 and 13 – reflectors of ultrasonic energy (pressure rolls); 5 – raw wire; 6 – magnetostrictive transducer; 7 – conical concentrator; 8 – nodal flange; 9 – frame of the classical drawing device; 10 – guide for ultrasonic waves; 11 – die; 12 – processed wire; A – amplitude of die's oscillations; B – wave oscillation at the level of the oscillation system as an assembly; C – waves oscillation in raw wire; D – waves oscillation in processed wire; — progressive wave; - - - regressive wave.

The U.Z.G. 2-4M-type ultrasonic generator, with a power of 2000 W and resonance frequency $f = 17.5 \times 10^3$ Hz, works in conjunction with the P.M.S. 15A-18-type oscillating system, which comprises a magnetostrictive transducer and a conical wave concentrator made from titanium-based alloy [4]. At the right side of the conical concentrator a guiding device for ultrasonic waves is screwed, in which the die was hot pressed. The die has tungsten carbide core and convergent conical inner geometry with semi angle conicity $\alpha = 8^\circ$ and cylindrical calibration zone. As drawing lubricant soap powder was used in a mixture with 10-15 % fine lime powder and 12-15 % talc powder.

The assembly of the oscillating system is dimensioned as a multiple of $\lambda/2$, where $\lambda = c/f$ is the ultrasonics wavelength determined by the ultrasonics propagation rate (c) in the metallic wire and resonance frequency (f).

The ultra-acoustic energy reflectors (pressure rolls) play the role to limit the action of ultrasonic energy upon well defined portions of both raw and processed wire, from AISI 52100 (RUL 1V/STAS 11250) ball bearing steel. Raw wire had initial diameter $D_0 = 4.6 \times 10^{-3}$ m and the chemical composition Fe-1.2 C-0.4 Mn-0.3 Si-1.5 Cr-0.02 S-0.02 P-0.08 Mo-0.2 Ni-0.2 Cu (wt. %). The wire was processed by single stage drawing to the final diameter $D_1 = 4.22 \times 10^{-3}$ m.

The research was focused on determining the influence of the ultrasonics oscillation amplitude (A) on the drawing force and on the mechanical characteristics of resistance and plasticity of the wires processed by UVD technology. In this purpose, both the cross-section reduction degree, $r = 100[1-(R_1/R_0)^2] \approx 16$ %, and the semi angle of die's conicity, $\alpha = 8^\circ$, were maintained constant. By a tuning procedure which was previously detailed [5] the ultrasonics oscillation amplitude was varied in three steps, $A = 5, 15$ and 20×10^{-6} m. Consequently, the maximum vibratory rate, $\bar{v}_v = 2 \pi f A$, became 0.55, 1.65 and 2.2 m/sec, respectively, which changed the ratio v_{dr}/\bar{v}_v , also called relative deformation rate to the values 0.54, 0.18 and 0.13, respectively, since $v_{dr} = 0.3$ m/sec was kept constant. The relative deformation rate influences the UVD friction coefficient, μ^{UVD} , in accordance with relationship (1). Therefore, the variation of ultrasonics oscillation amplitude influences the friction force at the metal-tool contact.

Four sets of five wire samples were used for each of the four single stage drawing tests performed by CT and by UVD with the above three ultrasonics oscillation amplitude, respectively. The measuring procedure of both technological and ultra-acoustic parameters was introduced in [2], each result being given as an average value of five tests performed in the same conditions on the samples from the same set.

The mechanical characteristics of resistance (yield stress, $R_{p0.2}$, and tensile strength, R_m) and plasticity (ultimate strain, A_5), were determined, for both raw and drawn wires, by tensile tests performed, according to EN 10002-1/1995, with a strain rate of 3.33×10^{-4} m/sec, on a MTS 810.24 tensile testing machine.

4. Experimental results and discussion

In the case of classical technology (CT), the experimental average value of the drawing force was determined as $F_{ex}^{CT} = 1370$ N. With this value, the experimental values were calculated for the drawing stress, $\sigma_{ex}^{CT} = 98$ MPa, by means of relationship (28) and for the friction coefficient, $\mu^{CT} = 0.026$, by means of Sach's relationship given in [2]. The effects of ultrasonics oscillation amplitude on both technological parameters and efficiency of UVD technology are summarized in Table 1.

Table 1. Effects of ultrasonics oscillation amplitude on both the technological parameters and the efficiency of UVD technology in case of processing AISI 52100 ball-bearing steel wires.

Ultrasonics oscillation amplitude at UVD technology	Technological parameters				UVD efficiency
	v_{dr}/\bar{v}_v	μ^{UVD}	F_{an}^{UVD} [N]	F_{ex}^{UVD} [N]	ΔF [%]
5×10^{-6} m	0.54	0.0062	1259	1250	8.75
15×10^{-6} m	0.18	0.0044	1205	1184	13.57
20×10^{-6} m	0.13	0.0030	1179	1147	16.27

Based on the value of the friction coefficient for classical technology, $\mu^{CT} = 0.026$, in column 3 the friction coefficients at UVD technology, μ^{UVD} , were calculated as a function of relative deformation rates v_{dr}/\bar{v}_v , by means of relationship (1). As compared to classical technology (CT), values at least four times lower were obviously obtained for UVD technology. The values of the analytical drawing force at UVD technology, F_{an}^{UVD} , were calculated in column 4 with relationship (28), based on the analytical drawing stress at UVD technology, σ_{an}^{UVD} determined with (27), where l is the length of the calibration zone of the die. Column 5 lists the experimental values recorded for

the drawing force at UVD technology, F_{ex}^{UVD} , which are in very good agreement with the analytical ones. Finally, the efficiency of UVD technology as compared to CT was determined in column 6 with the relationship: $\Delta F = 100[1 - (F_{ex}^{UVD} / F_{ex}^{CT})]$. It is obvious that the highest efficiency was obtained for the ultrasonics oscillation amplitude $A = 20 \times 10^{-6} m$, which gives the lowest relative deformation rate, in agreement with our previous observations [5].

The tensile stress-strain curves, determined as average values of five tests performed on raw (annealed) wires, on wires drawn with CT and on the three sets of wires processed by UVD are illustrated in Fig. 4.

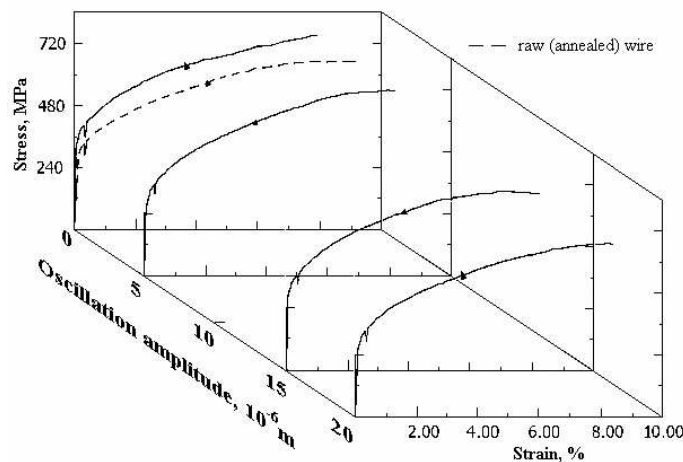


Fig. 4. Influence of the oscillation amplitude of ultrasonics at UVD technology on the tensile stress-strain curves of processed wires.

On one hand, in case of CT, designated by 0 oscillation amplitude, the drawn wires were obviously work hardened as compared to raw (annealed) wires. On the other hand, it is noticeable that, with the increase of ultrasonics oscillation amplitude, the decrease of intensity of the work hardening phenomenon in ultrasonically drawn wires occurs, which causes low mechanical characteristics of resistance and higher plasticity as shown in Table 2.

Table 2. Yield stress, ($R_{p0.2}$), tensile strength, (R_m) and ultimate strain, (A_5) of the curves from Fig. 4.

A, $10^{-6}m$	0		5	15	20
	raw wire	CT	UVD		
$R_{p0.2}$, MPa	332	401	370	349	327
R_m , MPa	650	746	711	685	667
A_5 , %	9.15	7.87	8.01	8.38	8.46

This diminution of the mechanical characteristics of resistance and increase of mechanical characteristics of plasticity, noticed at the wires processed by UVD as compared to those processed by CT, could be the caused, besides the surface effect of ultrasonics, by the so-called “effect of ultrasonic softening” acting in the oscillation nodes of both the raw and processed wire [6].

4. Conclusions

Based on a rate field with spherical distribution, a relationship was established for the drawing force for the metal wires and the analytical values were in very good agreement with the

experimental ones, determined at UVD processing of AISI 52100 (RUL 1V/STAS 11250) ball bearing steel wires.

With increasing ultrasonics oscillation amplitude applied to the die, from 5 to 20×10^{-6} m, progressive decreases were obtained of both the drawing force, from 1250 to 1147 N, and the friction coefficient, from 0.0062 to 0.003. As compared to classical technology, efficiencies higher than 16 % were obtained for UVD technology.

By tensile tests it was emphasised that UVD technology not only allows lower drawing forces but also reduces the work hardening level – a phenomenon which is always present in classical technology – causing increases of ultimate strain from 7.87 % at CT to 8.46 %.

Acknowledgements

Prof. M. Susan would like to thank Dr. C. Călin for his valuable expertise and supervision at the development of analytical relationships for the calculation of drawing force at UVD technology. This research was funded by Project no. 905/2000, National Program RELANSIN

References

- [1] E. Cazimirovici, M. Tarcolea, I. Negulescu, D. Raducanu, Teoria și tehnologia deformării prin tragere (roum.), (Theory and technology of the deformation by drawing) Technical Publ. House, Bucharest, pp. 97-101 (1990).
- [2] M. Susan, L. G. Bujoreanu, Rev. Metal. Madrid **35**, 379 (1999).
- [3] B. Avitzur, Wire Ind. 449 (1982).
- [4] M. Susan, Ph. D. Thesis, Faculty of Materials Science and Engineering, the “Gh.Asachi” Technical University Iași, 1996.
- [5] M. Susan, L. G. Bujoreanu, D. G. Gălușcă, C. Munteanu, V. Iliescu, Rev. Metal. Madrid 40 (2004), to be published.
- [6] R. Züst, Wire Ind. 341 (2000).